

Confinement of fermions in tachyon matter

Adamu Issifu^{1,*} and Francisco A. Brito^{1,2,†}

¹*Departamento de Física, Universidade Federal da Paraíba,
Caixa Postal 5008, 58051-970 João Pessoa, Paraíba, Brazil*

²*Departamento de Física, Universidade Federal de Campina Grande
Caixa Postal 10071, 58429-900 Campina Grande, Paraíba, Brazil*

In this paper we develop a phenomenological model inspired by QCD that mimics QCD theory. We use gauge theory in color dielectric medium ($G(\phi)$) coupled with fermion fields to produce scalar and vector confinement in *chromoelectric flux tube* scenario. Abelian theory will be used to approximate the non-Abelian QCD theory in a consistent manner. We will calculate vector and scalar glueballs and compare the result to the existing simulation and experimental results and projections. The QCD-like vacuum associated with the model will be calculated and its behavior studied relative to changing mass. We will also comment on the relationship between tachyon condensation, Higgs mechanism, QCD monopole condensation and their association with confinement. The behavior of the QCD string tension obtained from the vector potential of the model will be studied to establish vector dominance in confinement theories.

I. INTRODUCTION

Scalar and vector confinement [1] in $3 + 1$ dimensional world has been predicted by hadron spectroscopy [2], confinement in string picture and by QCD lattice simulation but no success has been made in solving it analytically from ‘first principle’ of QCD. It has been shown in quarkonia phenomenology in $3 + 1$ dimensional world that the best fit for meson spectroscopy are found for a convenient mixture of vector and scalar potentials. The combined vector and scalar potential has also been studied in many perspectives. Dirac equation [3] and Schwinger model [4] are among common examples employed to achieve both linear and coulomb-like potentials [5–9]. The attempt to confirm this result predicted by QCD lattice spectroscopy has led to the use of mass gap equation to generate mass as a dependent parameter even in quark systems with no mass current to create dynamic quarks [10]. Pure scalar and vector potentials have been dealt with in Refs.[11–15] as a point in focus.

In this work, we use the Lagrangian density for confinement of electric field in tachyon matter [16, 17] coupled with fermion fields [17] to produce a Lagrangian density for fermionic tachyons through transformations. In this approach, the dielectric function coupled to the gauge field and the fermion mass produce the needed strong interaction between (anti-) quark pairs and the scalar field ϕ describes the dynamics of the tachyons. We will use a dilaton in gauge theories [18] to determine the coupling constants of the colored particles by transforming the exponential dilaton potential to conform with our chosen tachyon potential considered in this work.

We show that both scalar and vector confinements coincide with the tachyon condensation. This phenomenon is not completely new because, tachyon fields play a role similar to Higgs fields where Higgs mechanism proceeds via tachyon condensation [19]. Again, both Higgs and tachyon fields have some properties in common, they are both associated with instability or fast decaying with negative square masses. The tachyons are expected to condense to a value of order of the string scale. Tachyons with large string couplings are considered charged, in that regard, their condensation leads to dual Higgs mechanism. This naturally translates into confinement in line with the QCD monopole condensation scenario [20]. Moreover, we will compute both vector and scalar glueball masses associated with the model. Glueballs are simply bound states of pure gluons, mixture of quark and gluon(hybrid) and multi quark bound states. The glueball spectrum has been a subject of interest for some decades now, with the focus on unraveling its states in the context of QCD theory [21].

The success of this type of confinement is based on *Nambu-Goto string* or the *chromoelectric flux tube picture*. The flux tube scenario is generally observed in static quark frame, such that there is no *chromomagnetic field* to induce the spin-orbit interaction of the quarks. The only interaction that is present, in this case, is the *kinematics Thomas spin-orbit interaction*, which is a relativistic correction. This is true for both vector and scalar confinement potentials and it is confirmed by lattice simulation results [23]. ‘*Thomas precession*’ is considered scalar, hence scalar potential is expected but it does not guarantee its connection with QCD theory. They only relate at long range spin-orbit

*Electronic address: bigadamsnet@yahoo.com

†Electronic address: fabrito@df.ufcg.edu.br

interactions of QCD, this is precisely the infrared (IR) regime of the theory. The vector potential is achieved for short range Thomas spin-orbit interaction and the scalar potential is consistent with long range Thomas spin-orbit interaction. Both models do not depend on the quarks' spin-orbit interactions in agreement with QCD theory [24]. Though, scalar potential models have been phenomenologically accepted and used in many hadron models, it is still struggling to plant its root firmly in fundamental QCD as highlighted in [22, 25]. Eventually, it was established that in a slowly moving quark frame, QCD predicts both spin dependent [30] and spin independent [29] relativistic corrections.

We will use an Abelian QED throughout the computations, but the color dielectric function $G(r)$ modifies the gauge field and by extension the QCD vacuum of the model [31, 32]. We will establish a relationship between the tachyon potential and the color dielectric function in a suitable manner. It is known that the Abelian part of the non-Abelian QCD string tension is 92%, this represents the linear part of the net potential. Thus, we can make an approximation of the non-Abelian field using an Abelian approach [33, 34]. Also, it is established that if Abelian projection is followed as suggested by 'tHooft, non-Abelian QCD is reduced to an Abelian theory with charges and monopoles occurring, when such monopoles condense, confinement results. The idea of monopole condensation is a very useful one. It has been numerically shown that monopole condensation actually occurs in the confinement phase of QCD [35]. Again, the color dielectric function coupled to the gauge field $F^{\mu\nu}F_{\mu\nu}$, contains only low momentum components. Therefore, the use of Abelian approximation is justified in phenomenological QCD theory. In sum, these properties enable us to apply phenomenological field theory for QCD in this investigation to establish confinement of quarks and gluons in the infrared regime [6, 36–38].

The color dielectric function G is responsible for the long distance dynamics that bring about confinement in the IR regime of the model. It also facilitates the strong interactions between quarks and gluons. The scalar field $\phi(r)$ is responsible for the dynamics of the self-interacting gluon fields and the color dielectric function. We will use a Lagrangian density that describes the dynamics of the gauge, the scalar field associated with the tachyon and gluon dynamics and fermion fields coupled with mass at zero temperature [38]. The motivation for using this approach are: Firstly, we are able to compute both the scalar and vector potentials by considering a heavy anti-quark source surrounded by a relatively light and slowly moving quarks. This enables us to compute the effect of short range spin dependent ‘*Thomas precession*’ (vector potential) and the effect of long range spin independent ‘*Thomas precession*’ (scalar potential). Secondly, we are able to apply phenomenological effective field theory to identify the color dielectric function with the tachyon potential in a simple form. Also, this approach makes it easy to observe how the QCD vacuum is modified by the dielectric function resulting in gluon condensation. Finally, vector and scalar glueball masses are easily calculated from the tachyon potential and the Lagrangian respectively.

The paper is organized as follows. In Sec. II we review the Maxwell's Lagrangian with source in color dielectric medium. In Sec. III we introduce the Lagrangian density for the model. In Sec. III A we derive the QCD-like vacuum of the model. In Sec. III B we choose a suitable tachyon potential for the study. In Sec. III C we compute the scalar and vector potentials for confinement, vector and scalar glueball masses and explore the physics involved. In Sec. IV we present the results and analysis. Our final comments are contained in Sec. V.

II. MAXWELL'S EQUATIONS MODIFIED BY DIELECTRIC FUNCTION

In this section we will review electromagnetic theory in *color dielectric medium*. Beginning with Maxwell's Lagrangian with source

$$\mathcal{L} = -\frac{1}{4}F_{\mu\nu}F^{\mu\nu} - j^\mu A_\mu, \quad (1)$$

its equations of motion are

$$\partial_\mu F^{\mu\nu} = -j^\nu. \quad (2)$$

The equations of motion of the electromagnetic field create spherical symmetric solutions similar to the well-known point charge scenario associated with Coulomb's field [40].

Therefore, for electromagnetic field immersed in a dielectric medium $G(\phi)$, where $\phi(r)$ is the scalar field representing the dynamics of the medium, we can construct a Lagrangian density

$$\mathcal{L} = -\frac{1}{4}G(\phi)F_{\mu\nu}F^{\mu\nu} - j^\mu A_\mu, \quad (3)$$

with its equations of motion given as

$$\partial_\mu [G(\phi)F^{\mu\nu}] = -j^\nu. \quad (4)$$

We choose the indices to run as $\mu = 1, 2, 3$ and $\nu = 0$. These choices are done carefully to obtain *chromoelectric flux* confinement and to eliminate *chromomagnetic fields* in the rest frame of the particles. As a result, the equation of motion in Eq.(4) can be reduced to

$$\nabla \cdot [G(\phi)\mathbf{E}] = j^0 = \rho. \quad (5)$$

By this equation, we have eliminated the effect of magnetic field contributions leaving only the electric field contributions that will run through this paper. From Eq.(5), \mathbf{E} is the electric field coupled to the dielectric function $G(\phi)$. Rewriting this equation in spherical coordinates, following the assumption that $E(r)$ and $\phi(r)$ are only functions of r , we get

$$\nabla \cdot [G(\phi)\mathbf{E}] = \frac{1}{r^2} \frac{\partial}{\partial r} (r^2 G(\phi) E_r) = \rho. \quad (6)$$

Integrating this differential equation yields

$$\begin{aligned} [r^2 G(\phi)\mathbf{E}] &= \frac{\rho}{\varepsilon_0} \int_0^R r^2 dr \\ E_r &= \frac{q}{4\pi\varepsilon_0 r^2 G(\phi)}, \end{aligned} \quad (7)$$

where $q = \frac{4}{3}\pi R^3 \rho$ and $E = |\mathbf{E}| = E_r$. We observe that the dielectric function modifies the magnitude of the electric field function.

III. LAGRANGIAN DENSITY OF THE MODEL

In this paper we will focus on a model described by a Lagrangian density given by

$$\mathcal{L} = -\frac{1}{4}G(\phi)F_{\mu\nu}F^{\mu\nu} + \frac{1}{2}\partial_\mu\phi\partial^\mu\phi - V(\phi) - \bar{\psi}(i\gamma^\mu\partial_\mu + q\gamma^\mu A_\mu - m_{q\bar{q}}G(\phi))\psi, \quad (8)$$

where $m_{q\bar{q}}$ is the bare fermion mass. It should be noted that due to the mass term together with gauge term, $F_{\mu\nu}F^{\mu\nu}$, the Lagrangian is certain to produce both scalar and vector potential contributions to the fermions. The equations of motion of this Lagrangian density are

$$\partial_\mu\partial^\mu\phi + \frac{1}{4}\frac{\partial G(\phi)}{\partial\phi}F^{\mu\nu}F_{\mu\nu} + \frac{\partial V(\phi)}{\partial\phi} - \bar{\psi}m_{q\bar{q}}\psi\frac{\partial G(\phi)}{\partial\phi} = 0, \quad (9)$$

$$-(i\gamma^\mu\partial_\mu + q\gamma^\mu A_\mu)\psi + m_{q\bar{q}}G(\phi)\psi = 0 \quad (10)$$

$$\partial_\mu[G(\phi)F^{\mu\nu}] = -\bar{\psi}q\gamma^\nu\psi. \quad (11)$$

Again the indices are $\nu = 0$ and $\mu = j = 1, 2, 3$ as defined in the previous section. These choices are made deliberately to avoid the creation of *chromomagnetic field* so we can focus on the *chromoelectric field* which creates the flux tube picture, relevant for our analysis. Therefore, Eq.(11) becomes

$$\nabla \cdot [G(\phi)\mathbf{E}] = \bar{\psi}q\gamma^0\psi = j^0 = \rho, \quad (12)$$

where we have substituted $F^{j0} = -E$. Expressing the above equation in spherical coordinates and integrating the results for electric field solution, yields the same result as Eq.(7).

Expanding Eq.(9) in radial coordinates to ease our analysis, we get

$$-\frac{1}{r^2}\frac{d}{dr}\left[r^2\frac{d\phi}{dr}\right] - \frac{1}{2}\frac{\partial G(\phi)}{\partial\phi}E^2 + \frac{\partial V(\phi)}{\partial\phi} - \bar{\psi}m_{q\bar{q}}\psi\frac{\partial G(\phi)}{\partial\phi} = 0. \quad (13)$$

Here we replace $F^{\mu\nu}F_{\mu\nu} = 2E^2$ and zero otherwise. This follows from the choice of indices defined above. For simplicity, we will also substitute ($\varepsilon_0 = 1$)

$$\lambda = \frac{q}{4\pi} \quad (14)$$

thus,

$$\frac{d^2\phi}{dr^2} + \frac{2}{r} \frac{d\phi}{dr} = -\frac{1}{2} \frac{\partial G(\phi)}{\partial \phi} \left[\frac{\lambda}{r^2 G(\phi)} \right]^2 + \frac{\partial V(\phi)}{\partial \phi} - \bar{\psi} m_{q\bar{q}} \psi \frac{\partial G(\phi)}{\partial \phi}, \quad (15)$$

which implies

$$\frac{d^2\phi}{dr^2} + \frac{2}{r} \frac{d\phi}{dr} = \frac{\partial}{\partial \phi} \left[V(\phi) + \frac{\lambda^2}{2} \frac{1}{V(\phi)} \frac{1}{r^4} - \bar{\psi} m_{q\bar{q}} \psi V(\phi) \right]. \quad (16)$$

It has already been established — see [41, 44] and references therein — that $G(\phi) = V(\phi)$ for slowly varying tachyons. This result will be used throughout this paper. In the above equation, if we consider a relatively large distance of particle separation from the charge q source, we can ignore the term with λ^2 , hence the equation reduces to

$$\nabla^2 \phi = \frac{\partial V(\phi)}{\partial \phi} [1 - q m_{q\bar{q}} \delta(\vec{r})]. \quad (17)$$

We have used the general definition $\bar{\psi}\psi = q\delta(\vec{r})$ in the above equation. Switching on the perturbation around the vacuum, $\phi_0 = 1/\alpha$, i.e. $\phi(r) \rightarrow \phi_0 + \eta(r)$, here $\eta(r)$ is a small fluctuation about the true vacuum of the potential, then as a result, Eq.(17) becomes

$$\begin{aligned} \nabla^2(\phi_0 + \eta) &= \frac{\partial V(\phi)}{\partial \phi} (1 - q m_{q\bar{q}} \delta(\vec{r})) \\ \nabla^2 \phi_0 + \nabla^2 \eta &= \left(\frac{\partial V}{\partial \phi} \Big|_{\phi_0} + \frac{\partial^2 V}{\partial \phi^2} \Big|_{\phi_0} \eta \right) (1 - q m_{q\bar{q}} \delta(\vec{r})) \\ \Rightarrow \nabla^2 \eta &= 4\alpha^2 (1 - q m_{q\bar{q}} \delta(\vec{r})) \eta, \end{aligned} \quad (18)$$

where in the last step we have used Eq. (17) for ϕ_0 and anticipated the property of the scalar potential that we shall define shortly.

A. Determining QCD-like Vacuum and Gluon Condensation

This section will be a continuation of the review under ‘Gluodynamics and QCD-like Vacuum’ contained in the first paper [44] in this series. We know that the Lagrangian for gluodynamics is symmetric under conformal transformation, when treated classically i.e. $|\epsilon_v| \rightarrow 0$. Without any quantum corrections, its energy-momentum tensor trace is zero, $\theta_\mu^\mu = 0$. As a result, it produces vanishing gluon condensate $\langle F^{\mu\nu} F_{\mu\nu} \rangle = 0$, in the classical limit and non-vanishing gluon condensate $\langle F^{\mu\nu} F_{\mu\nu} \rangle \neq 0$, with quantum corrections. Thus, quantum effects distorts the scale invariance [45] and brings about QCD energy-momentum tensor ($\theta^{\mu\nu}$) trace anomaly

$$\theta_\mu^\mu = \frac{\beta(g)}{2g} F^{a\mu\nu} F_{\mu\nu}^a, \quad (19)$$

a phenomenon well known in QCD theory. Here, $\beta(g)$ is the QCD beta-function of the strong coupling g , with a leading term

$$\beta(g) = -\frac{11g^3}{(4\pi)^2}. \quad (20)$$

This model produces vacuum expectation value

$$\langle \theta_\mu^\mu \rangle = -4|\epsilon_v|. \quad (21)$$

We will now compute the trace of the energy-momentum tensor from the Lagrangian Eq.(8) and compare the result with the result obtained above. This comparison is possible because, the third and the forth terms in Eq.(8) clearly breaks the scale invariant making it possible for comparison with Eq.(21). We calculate the energy-momentum tensor trace (θ_μ^μ) by substituting Eq.(9) into the expression

$$\theta_\mu^\mu = 4V(\phi) + \phi \square \phi, \quad (22)$$

and this yields,

$$\begin{aligned}
\theta_\mu^\mu &= 4V(\phi) - \phi \frac{\partial V}{\partial \phi} - \frac{\phi}{4} \frac{\partial G}{\partial \phi} F^{\mu\nu} F_{\mu\nu} + q\delta(\vec{r})m_{q\bar{q}}\phi \frac{\partial G}{\partial \phi} \\
&= 4\tilde{V}' + \tilde{G}' F^{\mu\nu} F_{\mu\nu} - 4q\delta(\vec{r})m_{q\bar{q}}\tilde{G}' \\
&= 4\tilde{V}'_{eff} + \tilde{G}' F^{\mu\nu} F_{\mu\nu}.
\end{aligned} \tag{23}$$

Here, we have redefined

$$\tilde{V}' = V - \frac{\phi}{4} \frac{\partial V}{\partial \phi}, \quad \tilde{G}' = -\frac{\phi}{4} \frac{\partial G}{\partial \phi} \quad \text{and} \quad \tilde{V}'_{eff} = \tilde{V}' - q\delta(\vec{r})m_{q\bar{q}}\tilde{G}'. \tag{24}$$

Comparing this Eq.(23) to Eq.(21) we get

$$\langle \tilde{G}'(\phi) F^{\mu\nu} F_{\mu\nu} \rangle = -4\langle |\epsilon_v| + \tilde{V}'_{eff}(\phi) \rangle. \tag{25}$$

We rescale $\tilde{V}'_{eff}(\phi)$ to include the vacuum energy density $-|\epsilon_v|$, i.e.,

$$\tilde{V}'_{eff} \rightarrow -|\epsilon_v|\tilde{V}'_{eff}, \tag{26}$$

consequently,

$$\langle \tilde{G}'(\phi) F^{\mu\nu} F_{\mu\nu} \rangle = 4|\epsilon_v|\langle \tilde{V}'_{eff} - 1 \rangle. \tag{27}$$

This equation follows the classical limit, where the gluon condensate vanishes when $|\epsilon_v| \rightarrow 0$ [53]. Again, we will demonstrate in the subsequent sections that, the gluon condensate increases with mass and remains non vanishing at $m_{q\bar{q}} = 0$, i.e. when the quark mass is ‘removed’ after confinement. This is a consequence of *chromoelectric flux tube* confinement.

B. Choosing The Appropriate Tachyon Potential

We select a suitable tachyon potential

$$V(\phi) = \frac{1}{2}[(\alpha\phi)^2 - 1]^2, \tag{28}$$

which produces tachyon condensation at low energies. This potential follows the restriction

$$V(\phi = \phi_0) = 0, \quad \frac{\partial V}{\partial \phi}|_{\phi=\phi_0} = 0 \quad \text{and} \quad \frac{\partial V}{\partial \phi}|_{\phi=0} = 0. \tag{29}$$

These restrictions are necessary to stabilize an asymptotically free system as well as its vacuum [54]. To proceed with the computations, we will require a suitable definition of the three dimensional Dirac delta function ($\delta(\vec{r})$) that appears in Eq.(18). Consequently, we define $\delta(\vec{r})$ in the limit of step function as [27]

$$\delta(\vec{r}) = \begin{cases} \frac{1}{4\pi} \lim_{R \rightarrow 0} \left(\frac{3}{R^3} \right), & \text{if } r \leq R \\ 0, & r > R \end{cases}, \tag{30}$$

where R is the radius of the hadron and r is the inter-particle separation distance. Solving Eq.(18) in the region $r \leq R$, i.e. we are considering the presence of the particles inside the hadron, we get

$$\eta''(r) + \frac{2}{r}\eta'(r) + 2K\eta(r) = 0, \tag{31}$$

where $K = 2 \left(\frac{3qm_{q\bar{q}}}{4\pi R^3} - 1 \right) \alpha^2$. This equation has a solution in the form

$$\eta(r) = \frac{\cosh(\sqrt{2|K|}r)}{r\alpha\sqrt{|K|}}, \quad \text{for } r \leq R, \tag{32}$$

where $|K| = -K = 2 \left(1 - \frac{3qm_{q\bar{q}}}{4\pi R^3}\right) \alpha^2$. Outside the hadron, $r > R$, $\delta(\vec{r}) = 0$, we have

$$\eta''(r) + \frac{2}{r}\eta'(r) + 2K_0\eta(r) = 0, \quad (33)$$

where $K_0 = -2\alpha^2$, which has a solution

$$\eta(r) = \frac{\cosh(\sqrt{2|K_0|r})}{\alpha r \sqrt{|K_0|}}, \quad \text{for } r > R. \quad (34)$$

Since our interest in this work is limited to confinement of the quarks and gluons inside the hadron, we will focus our attention on the solution obtained in the region $r \leq R$ (inside the hadron) represented by Eq.(32). The color dielectric function for this solution takes the form

$$\begin{aligned} G(\phi_0 + \eta) &= V(\phi_0 + \eta) = V(\phi)|_{\phi_0} + V'(\phi)|_{\phi_0}\eta + \frac{1}{2}V''(\phi)|_{\phi_0}\eta^2 + \mathcal{O}(\eta^3) \rightarrow \\ G(\eta) &= V(\eta) = \frac{1}{2}V''(\phi)|_{\phi_0}\eta^2. \end{aligned} \quad (35)$$

Tachyon fields are generally unstable with negative square masses therefore it is a common phenomenon to find their vacuum states being unstable. In this case, we choose a potential whose true vacuum is at $V(\phi)|_{\phi_0} = 0$. Switching on perturbation expansion about ϕ_0 , will results in a generation of square mass proportional to $V''(\phi)|_{\phi_0}$. This stabilizes the tachyon fields and reduce their velocities significantly, making them viable for analysis in the infrared (IR) regime of the model. Simply put, tachyon fields are naturally associated with instability in quantum field theory hence, we perturb the fields about its true vacuum where the potential has its minima. As a result, our perturbation should be understood as a mechanism to stabilize the tachyon fields [26]. Following from the above equation, the color dielectric function becomes

$$\begin{aligned} G(\eta) &= 2\alpha^2\eta^2 \\ &= \frac{2}{|K|r^2} \cosh^2(\sqrt{2|K|r}). \end{aligned} \quad (36)$$

Substituting the above result for $G(\phi)$ into the electric field equation in Eq.(7) we get

$$\begin{aligned} E &= \frac{\lambda}{r^2 G} \\ &= \frac{\lambda}{r^2 \left[\frac{2}{r^2 |K|} \cosh^2(\sqrt{2|K|r}) \right]}. \end{aligned} \quad (37)$$

The same tachyon potential and procedure adopted here was used in the first paper in this series — see reference [44] — to confine light quarks at a finite temperature. Consequently, the tachyons are expected to generate mass at $V''(\phi)|_{\phi_0}$ leading to a particle-like state resulting in tachyon condensation. It follows that, the vacuum stability is independent of the bare quark mass appearing in the Lagrangian density. These properties observed from this type of potential makes it more efficient for computing confinement potentials and glueball masses for heavy or light (anti-)quark systems. Following the afore analysis, we can associate $f_\alpha = 1/\alpha$ to the *decay constant* of the tachyons, the higher its value the faster the tachyons decay and by extension, the more unstable the QCD-like vacuum created in this process and the vice versa.

C. Vector Potential, Scalar Potetial and Glueball masses

1. Vector Potential

Using the well-known relation for calculating electromagnetic potentials

$$V_c(r) = \mp \int E dr, \quad (38)$$

to determine the confinement potential $V_c(r, m_{q\bar{q}})$, we get

$$\begin{aligned} V_c(r, m_{q\bar{q}}) &= \mp \frac{\lambda \sqrt{|K|} \tanh[\sqrt{2|K|}r]}{2\sqrt{2}} + c \\ &= \mp \frac{\lambda \sqrt{(1 - \beta q m_{q\bar{q}})} \tanh[\sqrt{4(1 - \beta q m_{q\bar{q}})}r]}{2} + c, \end{aligned} \quad (39)$$

where β is a constant representing the depth of the delta function well, i.e. $\beta = 3/4\pi R^3$. The above equation gives the net potential observed by massive (anti-)particle pairs ((anti-)quark pairs). In effect, particles of the same kind (two particles or two anti particles) repel each other whilst particles of different kinds (particle and anti-particle) attract; for example, color (blue) attracts an anti-color (anti-blue) of the same kind or colors of different kinds (blue and green) attracts each other and the vice versa [11].

We choose the negative part of the potential which correspond to the potential of an anti-particle. It is appropriate to choose $q = -1$ also corresponding to an anti-charge. We will later find that $q = -1$ is associated with an anti-charge which is identifiable with an anti-color charge carried by the gluons. Considering that, we are dealing with the potential of an anti-particle, this choice is justifiable. Also, we will choose $\beta = 1$ and $c = 0$ (c is the integration constant). Consequently, the vector potential seen by an anti-particle in the region $r \leq R$, in the rest frame of a heavy source is given by

$$V_c(r, m_{q\bar{q}}) = -\frac{\lambda \sqrt{(1 + m_{q\bar{q}})} \tanh[\sqrt{4(1 + m_{q\bar{q}})}r]}{2}. \quad (40)$$

Its QCD string tension σ is given as

$$\sigma(m_{q\bar{q}}) = -\lambda(m_{q\bar{q}} + 1). \quad (41)$$

This result corresponds to the short range Thomas spin-orbit interactions as highlighted in the introduction. We also find that there are spinless quarks (comparatively light) in a slow motion around the heavy point-like anti-quark source at the origin. The co-motion of the light quarks relative to the central massive static anti-quark source creates spin dependent corrections at short ranges. This produces a vector-type interactions resulting in a net vector potential as computed above [28]. To this end, when the surrounding co-moving quarks are far away from the heavy source, the string tension that binds them to the massive anti-quark source will break leading to pair production (a (anti-)quark pair creation), a phenomenon well known in QCD theory. However, in the presence of a heavy anti-quark source, the new quark created in the process remains attractive towards the original source whereas the new anti-quark created in the process remains attractive towards the ‘break-away’ quark. In this regard, the (anti-)quark pairs will always remain confined once there exist, at least, a heavy source. The process remains the same if we consider a heavy quark source as well. This characteristic is depicted by the linear nature of the string tension changing with $m_{q\bar{q}}$ and constant when $m_{q\bar{q}} = 0$.

2. Scalar Potential

To determine the resulting scalar potential seen by the quarks, we compare our results from Eq.(10) with the generalized Dirac equation where the scalar and the vector potentials may coexist as

$$[c\hat{\alpha}\hat{p} + \hat{\beta}m_0c^2 + V(r)]\psi = 0. \quad (42)$$

Here, we have used $P^\mu = (\frac{E}{c}, \vec{P})$, $A^\mu = (\Phi(r), \vec{A})$, but assumed scalar (spinless) and static quarks $E = \vec{A} = \Phi(r) = 0$. In spherical wall potential, we can impose the restriction

$$V(r) = \begin{cases} S(r), & \text{for } r \leq R \\ 0, & \text{for } r > R \end{cases},$$

where r is the inter-quark separations and R is the radius of the hadron. Here, $V(r) = S(r)$ represents the scalar potential in the Dirac equation. Thus, Eq.(42) can be rewritten as

$$(c\hat{\alpha}\hat{p} + \hat{\beta}m_0c^2)\psi + S(r)\psi = 0, \quad (43)$$

where $\hat{\alpha}$ and $\hat{\beta}$ are Dirac matrices. Also, $\hat{p} \rightarrow -i\nabla$ ($\hbar = 1$) is the momentum operator, m_0 is the rest mass of the fermions and c is the speed of light in vacuum. The vector potential is normally introduced by minimal substitution

of the momentum $P_\mu \rightarrow P_\mu - gA_\mu$ whilst the scalar potential is introduced by the mass term $m \rightarrow m_0 + S$, g is a real coupling constant. It should be noted that the vector and scalar potentials are coupled differently in the Dirac equation [47]. Comparing Eq.(10) and Eq.(43), we can identify the first and second terms of both equations as the interaction terms and the third terms as the scalar potentials [46, 48]. We leave out the vector potential because it has already been calculated in Sec. III C 1 so, it is of no further interest. The resulting scalar potential seen by the fermions is

$$S(r, m_{q\bar{q}}) = m_{q\bar{q}}G(r) = \frac{1}{2}m_{q\bar{q}}V''(\phi)|_{\phi_0}\eta^2(r) = 2m_{q\bar{q}}\alpha^2\eta^2 = m_{q\bar{q}}\left[\frac{2}{r^2|K|}\cosh^2(\sqrt{2|K|r})\right]. \quad (44)$$

This result represents Thomas spin-orbit interactions at long ranges where the short range Thomas spin-orbit interactions are partially dominated giving way to scalar interactions only. As a result, the interactions are thought of as being concentrated on the various quark nodes. Interestingly, the *scalar potential energy* is simply a product of $m_{q\bar{q}}$ and the color dielectric function. This gives an indication that confinement in this scenario has a direct relation with tachyon condensation and $m_{q\bar{q}}$ of the system.

Meanwhile, some authors have predicted vector dominance over scalar for inter quark potentials, suggesting that scalar dominance will imply all quark combinations are confined. Contrary to that, only the energetic combinations are preferred phenomenologically [11]. Therefore, we will attempt to analyze this assertion by computing and comparing the magnitudes of their coupling constants as they are expected to appear in the Dirac equation and its significance. Secondly, we will compare both the vector and the scalar potentials at increasing mass, decreasing mass and at zero mass to determine their strengths.

3. Glueball Masses

This model is certain to produce both vector and scalar glueballs just as vector and scalar potentials calculated above. Scalar glueball mass has been estimated to have a value within the range 1.5 to 1.7 GeV. This value has been affirmed by data and calculations [55]. Specific value was reached in Ref. [56] to be 1.7 GeV for fitness, through unquenched calculation. On the other hand, the existence of vector glueball mass has been predicted with an estimated value of 3.8 GeV by quenched Lattice QCD [57]. The vector glueball masses are expected to be observed at the ongoing Beijing Spectrometer Experiment (BESIII) and hopefully future PANDA experiment at the FAIR Lab [58]. Recent findings published by BESIII facility [59] points to vector particles of mass 3.77 to 4.60 GeV with precision. From the tachyon potential in Eq.(28) we can directly calculate the ‘vector glueball’ mass (m_{gb}) as

$$m_{gb}^2 = \frac{\partial^2 V}{\partial \phi^2}|_{\phi_0} = 4\alpha^2. \quad (45)$$

The scalar glueball mass is then calculated directly from the Lagrangian in Eq.(8) as

$$m_{gb\phi}^2 = -\left\langle \frac{\partial^2 \mathcal{L}}{\partial \phi^2} \right\rangle|_{\phi_0} = 4\alpha^2(1 + m_{q\bar{q}}) + \alpha^2 \langle F^{\mu\nu}F_{\mu\nu} \rangle|_{\phi_0} \quad (46)$$

where, we have substituted $\psi\bar{\psi} = q\delta(\vec{r}) \rightarrow q\beta$, $q = -1$ and $\beta = 1$. Following the analysis in Sec. III A, we find that $\langle F^{\mu\nu}F_{\mu\nu} \rangle|_{\phi_0} = 0$. Therefore, the model produces vanishing gluon condensate in its vacuum (ϕ_0). We can now rewrite Eq.(46) in terms of the string tension σ and the vector glueball mass as,

$$m_{gb\phi}^2 = m_{gb}^2\sigma. \quad (47)$$

From the afore discussions, we find that the vector and the scalar potentials are independent on the tachyon decay constant, $\alpha = 1/f_\alpha$. On the contrary, the glueball masses are dependent on the decay constant of the tachyons. Knowing the estimated values of scalar and the vector glueball masses and the value of the string tension $\sqrt{\sigma} = 420$ MeV [56] we can fix the tachyon decay constant within the range, $0 < f_\alpha \leq 1$. If we consider that the tachyons are decaying at half of its maximum value, i.e. $f_\alpha = 0.5$, we obtain $m_{gb\phi} = 1.68$ GeV and $m_{gb} = 4$ GeV. These values are within the range of the predicted values by lattice simulations. Consequently, the scalar and the vector glueball masses decrease with increasing tachyon decay and vice versa. As a results, glueball masses are more likely to be formed or observed at low energies in the IR regime.

D. Identification of Coupling Constants

In this section, we will compare the result from equation (16) with the well-known phenomenological models [11, 42], using dilaton in gauge theory to confine quarks and gluons with N_c colors. For emphasis, since our model

is phenomenological, it lacks all the degrees of freedom required to fully represent pure QCD theory, but our results agree with the QCD spectrum for scalar and vector potentials.

The results presented above still keeps the electromagnetic charge q and do not contain the color numbers N_c . This comparison is intended to help fill in these gaps. Furthermore, the scalar and the vector potentials in Dirac equation are of the same weight but coupled differently. This comparison will enable us to determine their couplings and relate them to their individual strengths in the QCD-like model. The same method was used in [41] — and references therein — to determine couplings as well. The dilaton model is given as

$$\frac{d^2\phi}{dr^2} + \frac{2}{r} \frac{d\phi}{dr} = -\frac{g^2}{64\pi^2 f_\phi} \left(1 - \frac{1}{N_c}\right) \exp\left(-\frac{\phi}{f_\phi}\right) \frac{1}{r^4} - \frac{\xi}{2f_\phi} \exp\left(-\xi \frac{\phi}{2f_\phi}\right) m_{q\bar{q}} g \delta(\mathbf{r}). \quad (48)$$

Transforming the exponential potentials of the above equation to conform with the tachyon potential used, i.e., $\exp\left(-\frac{\phi(r)}{f_\phi}\right) \rightarrow 2(\alpha^4 \phi^3 - \alpha^2 \phi)$ and $\exp\left(-\xi \frac{\phi(r)}{2f_\phi}\right) \rightarrow 2\left(\frac{\alpha^4 \phi^3 \xi^4}{16} - \frac{\alpha^2 \phi \xi^2}{4}\right)$, hence equation (48) can be rewritten as

$$\frac{d^2\phi}{dr^2} + \frac{2}{r} \frac{d\phi}{dr} = \frac{g^2}{32\pi^2 f_\phi} \left(1 - \frac{1}{N_c}\right) \frac{\alpha^2 \phi}{r^4} + \frac{2\xi^3 \alpha^2 \phi}{8f_\phi} m_{q\bar{q}} g \delta(\mathbf{r}). \quad (49)$$

It should be noted that the purpose of this section is to determine the coupling constants, so the equations have been simplified to achieve it.

Comparing equations (16) and (49), we can find $\xi = 2$, and $\alpha^2 = 1/f_\phi = 1/f_\alpha^2$. Here ξ represents the coupling strength of the fermions, f_ϕ is the mass decay constant of the dilaton and it is related to the decay constant of the tachyons f_α , g is the gluon charge and it is related to the electromagnetic charge q . We can rewrite equations (14), (40) and (41) as

$$\begin{aligned} \lambda &= -\frac{g}{2\pi} \left(1 - \frac{1}{N_c}\right)^{1/2} \Rightarrow \\ q &= -g \sqrt{\left(1 - \frac{1}{N_c}\right)}, \end{aligned} \quad (50)$$

$$V_c(r, m_{q\bar{q}}) = \frac{g}{4\pi} \sqrt{\left(1 - \frac{1}{N_c}\right)} \frac{\sqrt{(1 + m_{q\bar{q}})} \tanh[\sqrt{4(1 + m_{q\bar{q}})}r]}{2}, \quad (51)$$

and

$$\sigma(m_{q\bar{q}}) = \frac{g}{4\pi} \sqrt{\left(1 - \frac{1}{N_c}\right)} (m_{q\bar{q}} + 1) \quad (52)$$

for $g \rightarrow g/2\sqrt{2}$ respectively. Equation (35) can also be rewritten to reflect the afore couplings as

$$G(r, m_{q\bar{q}}) = 2\alpha^2 \eta^2 = \left[\frac{1}{r^2(1 + m_{q\bar{q}})} \cosh^2(2\sqrt{(1 + m_{q\bar{q}})}r) \right]. \quad (53)$$

We find from the above equation (53) for the dielectric function G that, the larger the quark mass the more stable the QCD-like vacuum and the faster the tachyons condense [43]. Since tachyon condensation implies confinement, then heavier quarks are more likely to confine than light quarks [49].

The *scalar potential energy* observed by the heavy anti-quark source is given as

$$S(r, m_{q\bar{q}}) = 2\alpha^2 \eta(r)^2 = m_{q\bar{q}} \left[\frac{1}{r^2(1 + m_{q\bar{q}})} \cosh^2(2\sqrt{(1 + m_{q\bar{q}})}r) \right]. \quad (54)$$

This potential follow the same analysis as the dielectric function, with the tachyons condensing faster in a multiple of $m_{q\bar{q}}$ showing a rather stronger confinement but vanishes at $m_{q\bar{q}} = 0$. This result represents the energy flow between a quark and an anti-quark pairs at long ranges. On the other hand, Eq.(51) represents the net *vector potential* for confinement observed for a heavy anti-quark source in the origin surrounded by relatively light spinless quarks in a slow motion.

It is important to state that, the potential seen in Eq.(51) corresponds to a mixture of $\xi = 0$ (no mass coupling) and $\xi = 1$ (Kaluza-Klein type or mass coupling) [50]. The combined $\xi = 1$ and $\xi = 0$ gives confinement of the quarks at all masses. Moreover, Eq.(54) gives the *scalar potential energy*, i.e., the flow of energy between two or more quarks. The coupling of the scalar potential, $\xi = 2$, exposes its weakness relative to the vector potential by a ratio of 1 : 2. By simple interpretation the weight of the scalar potential in the model constitutes 33% of the overall confinement potential. It is noticeable that the scalar potential vanishes at $m_{q\bar{q}} = 0$ while the vector potential does not. As a result, quarks are always in a confined state [52] under the vector potential at all masses but the scalar potential energy shows a degeneracy at $m_{q\bar{q}} = 0$. This is because the *chromoelectric flux* generated by the colored particles remain confined even if we ‘remove’ the quarks after confinement under the vector potential [2]. It should be noted also that, the net confinement of the colored particles is the sum of the vector and the scalar potentials combined.

After knowing all the coupling constants and the nature of the Dirac delta function, few comments on Sec. III A will be necessary. Noting that the Dirac delta function is well defined inside the hadron $r \leq R$, with depth $\beta = 3/(4\pi R^3) = 1$, $G(\phi) = V(\phi)$ and an anti-gluon color charge $q \rightarrow g = -1$ ($N_c \gg 1$), Eq.(24) takes the form

$$\begin{aligned}\tilde{V}'_{eff}(\phi) &= \tilde{V}' - q\delta(r)m_{q\bar{q}}\tilde{G}' \\ &= V - \frac{\phi}{4}\frac{\partial V}{\partial \phi} + m_{q\bar{q}}\left(-\frac{\phi}{4}\frac{\partial G}{\partial \phi}\right) \\ &= V - \frac{\phi}{4}\frac{\partial V}{\partial \phi}(m_{q\bar{q}} + 1)\end{aligned}\quad (55)$$

Substituting Eq.(35), recalling that $V(\eta(r)) = G(\eta(r)) = 2\alpha^2\eta^2$ for $\phi(r) \rightarrow \phi_0 + \eta(r)$, into the above expression yields

$$\begin{aligned}\tilde{V}'_{eff} &= 2\alpha^2\eta^2 - (\phi_0 + \eta)\alpha^2\eta(m_{q\bar{q}} + 1) \\ &= \alpha^2\eta^2(1 - m_{q\bar{q}}) - \phi_0\alpha^2\eta(1 + m_{q\bar{q}}) \\ &= \alpha^2\eta^2((1 - m_{q\bar{q}}) - \alpha\eta(1 + m_{q\bar{q}})) \quad \text{for} \quad \alpha = 1/\phi_0\end{aligned}\quad (56)$$

Since tachyon condensation is faster when $\tilde{V}'_{eff} \rightarrow 0$, see Fig. 3, tachyons condense with increasing mass and attain its minimum condensation at $m_{q\bar{q}} = 0$ corresponding to the maximum value of \tilde{V}' . As a results, Eq.(27) yields,

$$\begin{aligned}\langle(\phi_0 + \eta)G'(\eta)F_{\mu\nu}F^{\mu\nu}\rangle &= 16|\epsilon_v|\langle 1 - \alpha^2\eta^2(1 - m_{q\bar{q}})\rangle + 16|\epsilon_v|\langle \alpha\eta(1 + m_{q\bar{q}})\rangle \rightarrow \\ \langle(\alpha\eta + \alpha^2\eta^2)F_{\mu\nu}F^{\mu\nu}\rangle &= 4|\epsilon_v|\langle 1 - \alpha^2\eta^2(1 - m_{q\bar{q}})\rangle + 4|\epsilon_v|\langle \alpha\eta(1 + m_{q\bar{q}})\rangle.\end{aligned}\quad (57)$$

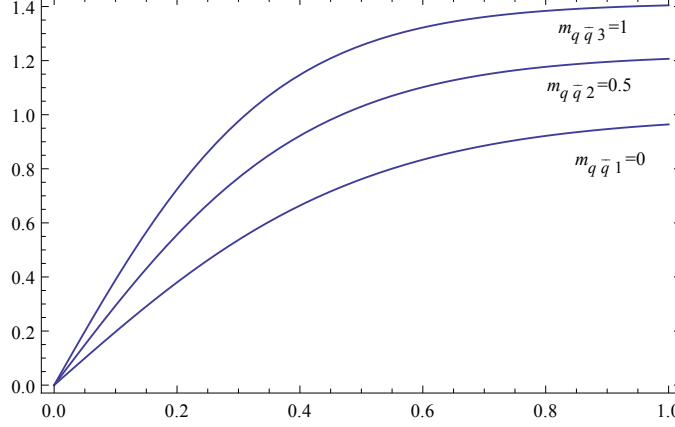
By this result, tachyon condensation increases with increasing mass $m_{q\bar{q}}$, and attain its minimum when $m_{q\bar{q}} = 0$. There is a QCD monopole condensation associated with both instances (i.e. $m_{q\bar{q}} = 0$ and $m_{q\bar{q}} > 0$), since the gluon condensate do not vanish in any of the two instances. The condensate is higher with increasing mass and relatively low at no mass. Naturally, confinement results in both instances.

IV. RESULTS AND ANALYSIS

Plotting the results of equations (51), (52), (53) and (54) in Fig. 1, Fig. 2, Fig. 3 and Fig. 4 we assume that $f_\alpha = \beta = \lambda = 1$, we get $g/4\pi = 1$ and $N_c \gg 1$. Fig. 1 shows graphically the relationship between the inter-quark potential $V_c(r, m_{q\bar{q}})$ with $(r, m_{q\bar{q}})$ for a heavy anti-quark source. The graph shows a steady increase in the gradient from $m_{q\bar{q}1}$ to $m_{q\bar{q}3}$ representing an increase in the strength of confinement from $m_{q\bar{q}1}$ to $m_{q\bar{q}3}$. Fig. 2 represents the graph of $\sigma(m_{q\bar{q}})$ against $m_{q\bar{q}}$, it shows a linear increase in $\sigma(m_{q\bar{q}})$ against $m_{q\bar{q}}$ with its foot intersecting the $\sigma(m_{q\bar{q}})$ axis at 1 indicating the strength of interaction even at $m_{q\bar{q}} = 0$. The linearity in $\sigma(m_{q\bar{q}})$ depict the confinement that exist between the (anti-) quark pairs. Fig. 3 shows the graph of the QCD-like vacuum which is equivalent to the tachyon potential. Tachyon condensation is related to monopole condensation which translates into confinement. The deeper the depth of the curve the more condensed the tachyons and the stronger the strength of the confinement and the vice versa. Again, Fig. 4 shows the relationship between the scalar potential $S(r, m_{q\bar{q}})$ with $(r, m_{q\bar{q}})$. We notice that the greater the quark mass the deeper the depth of the curve and the smaller the minima of the curves representing faster monopole condensation. As a result, the vector potential is stronger and more stable than the scalar potential for all masses. Considering all the factors discussed above, we can deduce that the vector potential is dominant over the scalar potential for a quark system.

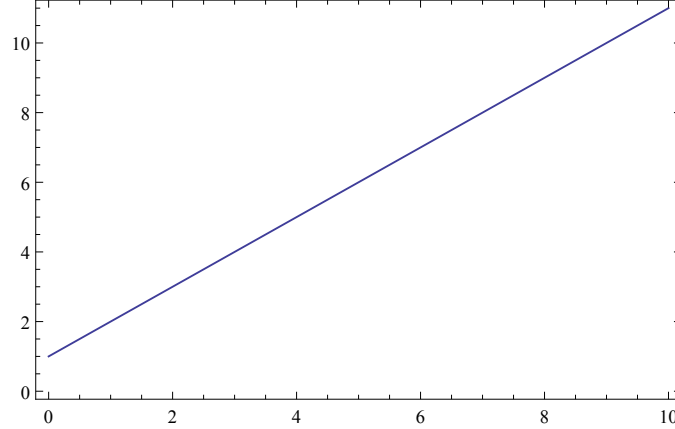
By way of analysis, we will compare the vector and the scalar confinement as captured in literature. The vector potential takes into account the angular momentum of the quarks whilst the scalar potentials do not. The scalar

FIG. 1: A graph of vector potential, $V_c(r, m_{q\bar{q}})$, against $(r, m_{q\bar{q}})$ for specific values of $m_{q\bar{q}}$.



The graph is for different values of $m_{q\bar{q}}$; $m_{q\bar{q}1} = 0$, $m_{q\bar{q}2} = 0.5$ and $m_{q\bar{q}3} = 1$. It shows the strength of $q\bar{q}$ confinement for different values of $m_{q\bar{q}}$ as their separation distances, r , vary. The graph shows a steady increase in its gradient as $m_{q\bar{q}}$ is increased from 0 to 1. By inference, the particles are strongly confined with increasing mass. That notwithstanding, a system of fermions remains confined even if the mass of the fermions vanishes ($m_{q\bar{q}} = 0$) due to the *chromoelectric flux tube confinement*, in consistency with the QCD theory.

FIG. 2: A graph of string tension $\sigma(m_{q\bar{q}})$ against mass, $m_{q\bar{q}}$, for a heavy anti-quark source.



The linear nature of the graph indicates that the $q\bar{q}$ is confined for increasing $m_{q\bar{q}}$. The foot of the graph at 1 shows that the particles remain confined even at $m_{q\bar{q}} = 0$ in consistency with QCD spectrum for heavy quarks.

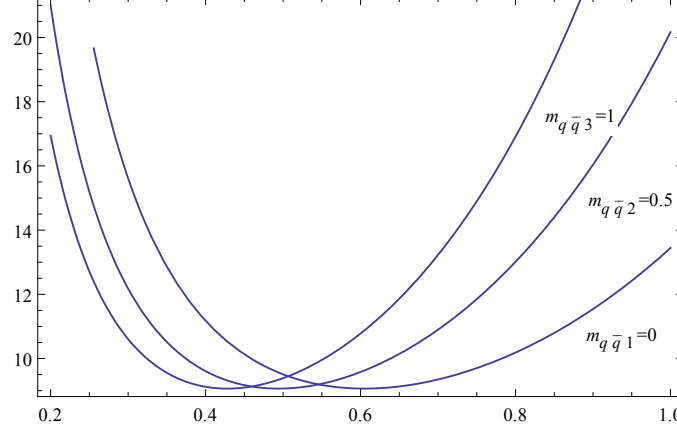
potential actually thrives on the basis that the angular momentum is partially eliminated. In the vector confinement, the energy of the quarks are carried by the gluons (string tension) whereas in the scalar confinement, the energy is centered on the quark coordinates. The scalar potential is most useful in a non rotating quark frames whilst the vector potential is a viable option for a rotating quark frames. Obviously, the ‘Thomas precession’ that gives rise to vector confinement differs significantly from the one that gives rise to the scalar confinement [3, 4, 23, 24].

V. CONCLUSIONS

The model gives an insightful detail about QCD theory making it more efficient for consideration. We have calculated the vector potential, scalar potential and the string tension associated with the vector potential. Vector and scalar glueball masses were also studied and their values for $f_\alpha = 0.5$ (consequently, $\phi_0 = 500\text{MeV}$), calculated and compared with the existing QCD lattice results for quenched (no quark fluctuation) and unquenched (hybrid fluctuation) approximations respectively.

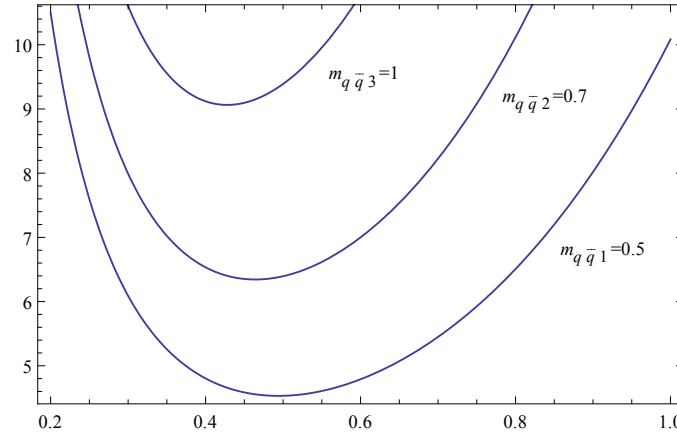
The dominance of the vector potential expected in QCD theory was clearly demonstrated by computing the coupling strengths ξ for both the vector and the scalar potentials. We estimated the weight of the scalar potential observed from the net confining potential of the model to be 33%. This was further justified by analyzing the graphs of the potentials at zero mass $m_{q\bar{q}} = 0$, all pointing to vector potential dominance. The vector and the scalar potentials should be understood as resulting from relativistic spin-orbit corrections at short and long ranges respectively. The

FIG. 3: A graph of color dielectric function, $G(r, m_{q\bar{q}})$, against $(r, m_{q\bar{q}})$ for specific values of $m_{q\bar{q}}$.



It is a graph of $m_{q\bar{q}1} = 0$, $m_{q\bar{q}2} = 0.5$ and $m_{q\bar{q}3} = 1$ to show how the tachyons condense with increasing mass. Even though we find some tachyon condensate at $m_{q\bar{q}} = 0$, we can also see that, the condensation is faster with increasing mass. The deeper the depth of the graph, the more condensed the tachyons are and the vice versa.

FIG. 4: A graph of the scalar potential $S(r, m_{q\bar{q}})$ against $(r, m_{q\bar{q}})$ for specific values of $m_{q\bar{q}}$.



The potential vanishes at $m_{q\bar{q}} = 0$, and increases in depth as $m_{q\bar{q}}$ increases.

vector potential shows confinement of *chromoelectric flux* at zero mass but the scalar potential vanishes at the same mass indicating its weakness. This makes the vector potential more suitable for confining light quarks. Furthermore, we established the relation between tachyon condensation, dual Higgs mechanism, QCD monopole condensation and confinement. Finally, we intend to continue our series on this subject by studying confinement of fermions at finite temperature.

Acknowledgments

We would like to thank CNPq and CAPES for partial financial support. FAB acknowledges support from CNPq (Grant no. 312104/2018-9).

-
- [1] S. Eidelman, B. K. Heltsley, J. J. Hernandez-Rey, S. Navas and C. Patrignani, arXiv:1205.4189 [hep-ex], (2012 Review).
 - [2] N. Brambilla et al., CERN-2005-005, (CERN, Geneva, 2005), arXiv:hep-ph/0412158.
 - [3] A. S. de Castro, *Phys.Lett. A* **305** (2002) 100-104; Erratum-ibid. *A* **308** (2003) **80**, [hep-th: 0209196].
 - [4] S. Coleman, R. Jackiw and L. Susskind, *Ann. Phys. (N.Y.)* **93**, 267 (1975).
 - [5] B. J. Harrington, S. Y. Park and A. Yildiz, *Phys. Rev. Lett.* **34** (1975) 168.
 - [6] E. Eichten, K. Gottfried, T. Kinoshita, J. Kogut, K. D. Lane and T.-M. Yan, *Phys. Rev. Lett.* **34** (1975) 369.

- [7] W. J. W. Muller-Kirsten, *Phys. Rev.* **D 12** (1975) 1103.
- [8] J. F. Gunion and R. S. Willey, *Phys. Rev.* **D 12** (1975) 174.
- [9] K. S. Jhung, K. H. Chung and R. S. Willey, *Phys. Rev.* **D 12** (1975) 1999.
- [10] P. Bicudo and G. M. Marques, (2003), arXiv:0309231 [hep-ph].
- [11] R. Dick, *Phys. Lett.* **B 409** (1997) 321;
- [12] W. Lucha et al., *Phys. Rep.*, **200** (1991) 127.
- [13] L. B. Castro, A. S. de Castro and M. B. Hott, *Eur. Phys. Lett.* **77** 20009 (2007).
- [14] M. Creutz, *Phys. Rev.* **D 21** (1980) 2308.
- [15] M. Luscher, K. Symanzik and P. Weisz, *Nucl. Phys.* **B 173** (1980) 365.
- [16] E. Majorana and N. Cimento, **14** (1937) 171.
- [17] P. A. M. Dirac, *Proc. Roy. Soc. (London)* **A 117** (1928) 610,
- [18] R. Dick, *Phys. Lett.* **B 397** (1997) 193.
- [19] A. Sen, **JHEP 08** (1998) 012, [hep-th/9805170],
H. J. Rothe, "Lattice Gauge Theories", (World Science, 1992).
- [20] O. Bergman, K. Hori and P. Yi, *Nucl. Phys.* **B 580** (2000) 289-310.
- [21] V. Mathieu, N. Kochelev and V. Vento, *Int. J. Mod. Phys.* **E18** 1 49(2009),
M. Rosina, A. Schuh and H.J. Pirner, *Nucl. Phys.* **A 448**, 557 (1986).
- [22] A.B. Henriques, B.H. Kellet, and R.G. Moorhouse, *Phys. Lett.* **B 64**, 85 (1976)
- [23] G.S. Bali and P. Boyle, *Phys. Rev. D* 59, 114504 (1999).
- [24] N. Brambilla and B.M. Prospero, *Phys. Lett.* **B 236**, 69 (1990). Collin Olson, M.G. Olsson, and Ken Williams, *Phys. Rev.* **D 46**, 4307 (1992).
- [25] Theodore J. Allen, M. G. Olsson and S. Veseli, *Phys.Rev.* **D 62** 094021 (2000)
- [26] Maxime Gabella, 'Tachyon Condensation in Open String Field Theory' University of Oxford, Spring 2008.
- [27] Sydney Geltman, *Mol. and Opt Phys.*, 573179, (2011).
- [28] T.J. Allen, M.G. Olsson, S. Veseli, and K. Williams, *Phys. Rev.* **D 55**, 5408 (1997).
- [29] A. Barchielli, E. Montaldi and G.M. Prospero, *Nucl. Phys.* **B 296**, 625 (1988); **303**, 752(E) (1988); A. Barchielli, N. Brambilla and G.M. Prospero, *Nuovo Cimento* **A 103**, 59 (1989).
- [30] E. Eichten and F. Feinberg, *Phys. Rev.* **D 23**, 2724 (1981); D. Gromes, *Phys. Rev.* **C 22**, 265 (1984).
- [31] L. Wilets, 'Non topological solutions', world Scientific, Singapore, 1998.
- [32] T. D. Lee, 'Particle physics and introduction to field theory, Harwood Academic, New York, 1981.
- [33] H. Shiba et al, *Phys. Lett*, **B 333** 461 (1994).
- [34] G. S Bali et al. *Phys. Rev.* **D 54**, 2863 (1996).
- [35] Tsuneo Suzuki, *Prog. Theor. Phys.* Vol. 81, NO. 4, (1989) Progress letters.
- [36] A. Chodos, R. L. Jaffe, K. Johnson, C. B. Thorn and V. F. Weisskopf, *Phys. Rev.* **D 9** 3471 (1974).
- [37] W. A. Bardeen, M. S. Chanowitz, S. D. Drell, M. Weinstein and T. M. Yan, *Phys. Rev.* **D 11** 1094 (1994).
- [38] R. Friedberg and T. D. Lee, *Phys. Rev.* **D 15** 1964 (1997).
- [39] A. Sen, **JHEP 0207** 065 (2002) [hep-th/0203265];
A. Sen, **JHEP 0204** 048 (2002) [hep-th/0203211].
- [40] M. Cvetič and A. A. Tseytlin, *Nucl. Phys.* **B 416** 137 (1994).
- [41] F. A. Brito, M. L. F. Freire and W. Serafim, *Eur. Phys. J. C.* (2014) **74** 3202.
- [42] O. Adreiev and V. I. Zakharov, *Phys. Lett.* **B 645** 437 441 (2007).
- [43] R. Jackiw, *Phys. Rev.* **D 9** 1686 (1974).
- [44] A. Issifu and F. A. Brito, *Adv. High Energy Phys.* **2019**, 9450367 (2019) doi:10.1155/2019/9450367 [arXiv:1706.09013 [hep-th]].
- [45] J. Ellis, *Nucl. Phys.* **B22** (1970) 478; R.J. Crewther, *Phys. Lett.* **B33** (1970) 305, *Phys. Rev. Lett.* **28** (1972) 1421; M.S. Chanowitz and J. Ellis, *Phys. Lett.* **B40** (1972) 397; *Phys. Rev.* **D7** (1973) 2490.
- [46] H.-W. Ke, Z. Li, J.-L. Chen, Y.-B. Ding and X.-Q. Li, *Int.J.Mod.Phys.* **A 25** 1123 (2010) 1134.
- [47] A. D. Alhaidari, H. Bahloul and A. Al-Hasan, *Phys.Lett.* **A 349** (2006) 87 97.
- [48] W. Greiner, *Relativistic Quantum Mechanics*, Springer, Berlin (2000).
- [49] M. J. Strassler, 'On Confinement Duality', (University of Pennsylvania, Philadelphia, USA, 2001).
- [50] M. Thorsrud, "Quintessence with Kaluza-Klein type couplings to matter and an isotropy-violating vector field", arXiv:1303.2469 [gr-qc].
- [51] E. Eichten et al., *Phys. Rev.* 17 (1978) 3090; *Phys. Rev.* **D 21** (1980) 203
- [52] H. Suganuma, S. Sasaki and H. Toki, *Nucl. Phys.* **B 435** (1995) 207.
H. Suganuma, S. Sasaki and H. Toki, *Pro. of Int. Conf. on "Quark confinement and Hadron Spectrum"*, Como Italy, (World Scientific, 1993).
H. Tiko, H. Suganuma and S. Saaki, *Nucl. Phys.* **A 577** (1994) 353c.
S. Sasaki, H. Suganuma and H. Tiko, preprint, **RIKEN-AF-NP 172** (1994).
- [53] D. Kharzeev, E. Levin and K. Tuchin, *Phys. Lett.* **B547** 2130 (2002).
- [54] M. Rosina, A. Schuh and H. J. Pirner (1986). *Nucl. Phys.* **A 448** 4 557(1986)566.
- [55] M. R. Pennington, workshop on photon Interactions and the Photon Structure (Lund, Sweden, 1998), hep-ph/9811276.
- [56] J. Sexton, A. Vaccarino and D. Weingarten, *Phys. Rev. Lett.* **75**, 4563 (1995).
- [57] Y. Chen, A. Alexandru, S. J. Dong, T. Draper, I. Horvath, F. X. Lee, K. F. Liu and N. Mathur et al., *Phys. Rev.* **D 73**, 014516 (2006) [arXiv:hep-lat/0510074].

- [58] F. Giacosa, J. Sammet and S. Janowski, Phys. Rev. **D 95**, 114004 (2017).
- [59] M. Ablikim, M. N. Achasov, S. Ahmed, X. C. Ai, O. Albayrak, M. Albrecht, et al., Phys. Rev. Lett. **118** 9 (2017).